Supplementary Materials for

Dermal sheath contraction powers stem cell niche relocation during hair cycle regression

Nicholas Heitman, Rachel Sennett, Ka-Wai Mok, Nivedita Saxena, Devika Srivastava, Pieter Martino, Laura Grisanti, Zichen Wang, Avi Ma'ayan, Panteleimon Rompolas, and Michael Rendl*

*Corresponding author. Email: michael.rendl@mssm.edu

This PDF file includes:

Other Supplementary Materials for this manuscript includes the following:

Movies S1 to S3 (.avi)
Tables S1 and S2

Materials and Methods

Mice

Sox2^{GFP} (*35*) and *Lef1-RFP* (*26*) mice to label skin populations was described previously (*6, 27*). *R26*$^{mT/mG}$ (*36*), *Acan*^{CreER} (*37*), *R26*$^{LSL\text{-}tdTomato}$ (Ai14) (*38*), and *R26*$^{LSL\text{-}DTA}$ (*39*) were obtained from the Jackson Laboratory. Generation of *Tbx18*^{Cre} and *Tbx18*^{H2BGFP} mice was previously described (*31*). Generation of *K14-H2BCer* mice is described below. All animal studies were conducted in accordance with the guidelines and approval of the Institutional Animal Care and Use Committee (IACUC) at ISMMS, and all mice used in this study were housed in facilities operated by the Center for Comparative Medicine and Surgery (CCMS) at ISMMS.

Acan^{CreER}*;R26*$^{LSL\text{-}tdTomato}$ and *Acan*^{CreER}*;R26*$^{LSL\text{-}DTA}$ mice were injected with tamoxifen (20 mg/ml dissolved in corn oil, injections of 0.2 g/kg body weight i.p.) daily from P10-P12 for DS-labeling and -ablation experiments and P9, P10 for intravital imaging experiments. Animals were PCR genotyped to select for control and experimental groups without blinding. All labeling, ablation, and *intravital* imaging experiments were repeated with at least three different mice; all specific n values for each experiment were listed in figure legends. All experiments were performed on both sexes with verification of all major findings present in both, but only results from females were reported to avoid any variation of measurements owing to sex.

Human scalp samples

Samples of human scalp were obtained from the Skin and Laser Center of the Mount Sinai Health System. Samples were collected during Mohs procedures, and regions of healthy tissue were separated from tumor-containing regions before processing. Additionally, selected tissue was verified for the absence of tumors by histology before use in further experimentation. Personal patient information was blinded to researchers except for age and sex.

Generation of *K14-H2BCer* mice

An H2BmCerulean3 (H2BCer) insert was obtained from the mCerluean3-N1 plasmid (M. Davidson via Addgene, #54730) by BamHI/XbaI (NEB) restriction enzyme digestion and subsequently ligated into a pG3Z-K14-H2B vector (E. Fuchs) with T4 Ligase (NEB). The final K14-H2BCer cassette was obtained from the resultant plasmid by digestion with KpnI and SphI (NEB) and injected into blastocysts at the ISMMS Mouse Genetics and Gene Targeting CoRE. Transgenic mice were then screened by assessing Cer fluorescence in tail tips and PCR genotyping using primers targeting the transgene-unique *K14* promoter/enhancer. A single founder was then selected from all mice positive for the transgene that had the highest and most uniform expression of H2BCer in the epidermis of F1 generation mice to establish the final transgenic line.

Immunofluorescence and microscopy

For immunofluorescence on tissue sections, back skins were harvested then embedded and fresh frozen in OCT (Tissue Tek). Sections were cut at a thickness of 8 μm with a Leica cryostat. After drying, sections were post-fixed to slides with 4 % paraformaldehyde for 15 minutes at room temperature. After washing in PBS, sections were then permeabilized in 0.3-1.0 % Triton X-100/PBS for 15 minutes at room temperature before blocking in 0.5 % normal donkey serum (Jackson ImmunoResearch) or MOM blocking reagent for mouse primary antibodies (Vector Labs) for 1 hour at room temperature. Primary antibody labelling against ITGA8 (R&D Systems,

goat 1:100), ACAN (Millipore, rabbit 1:100), αSMA (1A4, Neomarkers, mouse 1:100), PDGFRA (eBiosciences, rat 1:100), ECAD (Invitrogen, rat 1:1000), LEF1 (Cell Signaling, rabbit 1:100), K14 (Gifts from J. Segre, rabbit or chicken 1:1000), activated CASP3 (R&D Systems, rabbit 1:300), Ki67 (Leica, rabbit 1:200), AE13 (Abcam, mouse 1:100), AE15 (Santa Cruz, mouse 1:50), K6 (Gift from E. Fuchs, rabbit 1:1000), MYH10 (Cell Signaling, rabbit 1:25), MLCK (Abcam, rabbit 1:100), MYL9 (Proteintech, rabbit 1:100), phosphorylated (Ser19) MYL9 (Novus, rabbit 1:100), or SM22 (Proteintech, rabbit, 1:200) was performed at room temperature for 1 hour or 4º C overnight. Secondary labeling was done with donkey anti-goat, rabbit, rat, or mouse antibodies conjugated with AlexaFluor 488, 555, or 647 (Jackson ImmunoResearch, Invitrogen) for 30 minutes at room temperature. Nuclei were labelled with Hoechst 33342 (Thermo Fisher), and stained sections were mounted in a glycerol-based p-phenylenediamine (Sigma) antifade reagent.

For whole mount immunofluorescence of single hair follicles from mouse back skin or human scalp, tissues were harvested and fixed in 4 % PFA for 2 hours at room temperature with gentle shaking. Individual hair follicles were then separated from the skin through microdissection under a Leica S6E stereomicroscope and collected into a 96-well plate with PBS. Tissue was permeabilized in 0.5 % Triton X-100/PBS for 15 minutes, washed, then stained in primary antibody against αSMA (Abcam, rabbit 1:300), K14 (Gift from J. Segre, rabbit 1:1000), SM22 (Proteintech, rabbit 1:200), MYH11 (Proteintech, rabbit 1:100), or MYL9 (Proteintech, rabbit 1:100) at 4ºC overnight. Secondary labeling was done with donkey anti-rabbit or chicken antibodies conjugated with AlexaFluor 488, 555, or 647. Nuclei were then labelled with Hoechst 33342, and follicles were then mounted in antifade reagent.

The whole mount immunofluorescence of pieces of intact back skin followed a modification of a previously published procedure (40). Tissues were harvested, and fixed in 4 % PFA for 2 hours at room temperature or overnight at 4º C before peeling away the panniculus carnosus muscle and cutting into 1 cm x 2 cm strips. Subsequent steps were then performed in a 6-well plate. Skins were then treated with 0.3 % Triton X-100/PBS for 8 hours before primary antibody staining for K14 (rabbit 1:1000) in a 0.3 % Triton X-100, 5 % donkey serum, 20 % DMSO/PBS solution at room temperature for 5 days with gentle shaking. After washing in 0.3 % Triton X-100/PBS solution for 8 hours at room temperature with media changes every 30 minutes, tissues were then stained with a donkey anti-goat AlexaFluor 555 antibody in the Triton X-100/donkey serum/DMSO/PBS solution used similarly with primary antibody labeling for 3 days at room temperature with gentle shaking. Finally, tissues were washed again in 0.3 % Triton X-100/PBS solution for 8 hours at room temperature with buffer changes every 30 minutes and counter stained with Hoechst 33342. Optical clearing was then performed by dehydrating tissue in 50:50 methanol/water for 5 minutes then a series of three 100% methanol treatments for 30 minutes each at room temperature. Final clearing was performed in a BABB (benzyl alcohol/benzyl benzoate, 1:2 ratio) solution until visibly clear then mounted in residual BABB held in a custom chambered glass slide.

Immunofluorescence stained sections were imaged with Leica DM5500 widefield microscope, and whole mount stained tissues were imaged with a Leica SP5 DMI confocal microscope equipped with Leica LASAF software. Images were post-processed and adjusted for brightness and contrast using ImageJ/FIJI (NIH). Hair follicle length was measured from whole mount fluorescence stained, cleared back skin in FIJI and defined as length from the proximal tip of K14+ epithelium to the base of the sebaceous gland.

Isolation of DS, DP, and DF

During morphogenetic anagen, DP and DS from 1st and 2nd wave hair follicles could be distinguished based on distinct expression patterns of *Sox2^{GFP};Lef1-RFP* reporter expression (*27*). In order to further purify the DS and DP both were selected as PDGFRA-Brilliant Violet 421+. Back skins were harvested from P5 mice and digested in dispase (Invitrogen) overnight at 4° C. Epidermis was then removed from dermis by peeling, and the dermis was then digested in a 0.2 % collagenase (Sigma-Aldrich) and DNase (20 U/µl, Roche) solution at 37° C for one hour with gentle shaking. Cell pellets were obtained by centrifugation at 350 x g for 5 minutes and further digested in 0.25 % trypsin EDTA solution for 5 minutes at 37° C. Cells were then stained against PDGFRA (eBiosciences, biotinylated rat, 1:50,) followed by streptavidin-Brilliant Violet 421 (Biolegend, 1:200) secondary staining. DAPI was added for live/dead cell identification and cells were sorted using a BD Influx cell sorter at the ISMMS Flow Core facility using the following criteria: DP = GFP$^+$, RFP$^+$, PDGFRA$^+$; DS = GFP$^+$, RFP$^-$, PDGFRA$^+$; DF = GFP$^-$, RFP^{mid}. FACS profiles were analyzed using FlowJo software.

qRT-PCR

Whole cell RNA was purified from sorted cells using the Absolutely RNA Nanoprep Kit (Agilent). cDNA synthesis was done with Superscript III (Invitrogen) using oligo(dT) primers. qRT-PCR was performed using SYBR Green Master Mix I (Roche) on a LightCycler 480 thermocycler (Roche). Relative mRNA levels were calculated using the 2-ΔΔCt method, normalized to *Gapdh*. All measurements were performed with biological duplicates each with technical duplicates. Gene specific primers are listed in table S3.

RNA sequencing and analysis

Total RNA was purified from sorted cells using the Absolutely RNA Nanoprep Kit (Agilent). RNA concentrations were measured with a NanoDrop spectrophotometer (Thermo), and quality was assessed using an Agilent Bio-analyzer. Samples with an RNA integrity number score of 8 or higher were further processed. 6 ng of starting material was reverse transcribed and amplified with the RNA Ovation RNAseq System V2 (NuGEN). cDNA was then sheared by sonication using a Covaris LE220. From 100 ng of sheared amplified cDNA, sequencing libraries were generating with 6 unique barcoded adaptors, one for each sample (2 biological replicates x 3 populations) using the Ovation Ultralow DR Library System (NuGEN). Library concentration and quality were quantified by Qubit (Invitrogen) and Agilent Bioanalyzer. Samples were then sequenced on the Illumina HiSeq 2000 platform using a 50-nt single-read setting at the Genome Technology Center at NYU.

To refine the DS gene signature, previously published RNA sequencing data from 3 additional follicle populations consisting of hair follicle outer root sheath, matrix, and melanocytes obtained at a similar age (*27*) were included in analyses. Raw RNA sequencing reads were mapped to the mm10 mouse genome with TopHat v2.0.3 (*41*) coupled with Bowtie2 (*42*) aligner with default parameters. Transcriptomes were assembled and fragments per kilobase per million reads (FPKM) for each gene were computed with Cufflinks v2.1.1 (*43*). Differentially expressed genes (DEGs) were identified using Cuffdiff (with default parameters except for the library normalization method was upper quartile normalization, where FPKMs were scaled via the ratio of the 75th quartile fragment counts to the average 75th quartile value across all libraries) and ANOVA with Benjamini-Hochberg correction for multiple hypothesis testing with significance cut off FDR < 0.05. Principal component analysis and hierarchical

clustering were performed on all DEGs using Origin 2019 (OriginLab) and Morpheus (Broad) respectively. Population signature genes were defined by DEGs with an FPKM ≥ 5, and fold enrichment ≥ 2 compared to all other populations. Gene set enrichment analysis was performed on GenePattern (Broad) using a user-defined gene set for smooth muscle contraction and regulation components (table S2).

Intravital live-imaging and analysis

Acan^{tdT}*;Tbx18*^{H2BGFP}*;K14-H2BCer* mice were injected with tamoxifen (0.15 g/kg i.p.) at P9 and P10 to label DS cytoplasm with tdT. Mice were then imaged at P15 or P16 to capture mid-regression using an Olympus FV1000 MPE 2-photon microscope equipped with a tunable Coherent Chameleon Ultra Ti:Sapphire laser. During imaging, mice were first anaesthetized with ketamine/xylazine mixture (100 mg/kg, 12.5 mg/kg i.p.) and subsequently maintained on inhaled isoflurane anesthetic (0.75 % isoflurane vapor, O2 flow rate = 0.75 L/minute, EZ Anesthesia) delivered through nose-cone. Specifications of the imaging stage set up was as previously described (*2, 15, 18, 44*). Optical slices were captured using a single 900 nm excitation wavelength at 10 % laser power and resultant fluorescence imaged with a 25X XLPlanLN water immersion objective (NA 1.05, Olympus). Emission filters for each channel were as follows: blue = BA420-456, green = BA495-540H, red = BA575-630. Each optical slice field had a 250 x 400 μm area captured at a resolution of 640 x 1024 px with a 12.5 μs/px scan speed. Z-stacks of 30-45 μm in depth were taken with 3 μm step intervals. Time intervals between acquisitions for time-lapse imaging were 7.5 minutes.

Raw images of time-lapse series were processed in FIJI to separate fluorescence signal from each fluorescent protein type, the process for which is demonstrated in fig. S11. Fluorescence signal captured by each channel were as follows: blue = mCerulean3 and second harmonic generation (SHG), green = GFP and Cer, and red = tdT and mCerulean3. The excitation/emission spectra and fluorescence strength of Cer permitted its fluorescence excited at 900 nm to be strongly visible in the blue and green channels and moderately visible in the red channel. To isolate only the Cer signal in the blue channel, first the pixel values of the green channel were subtracted from the blue channel to obtain SHG signal, which was then subtracted from the blue channel so that only Cer signal remained. The resulting Cer pixel values were then subtracted from the green and red channels to isolate GFP and tdT signal respectively. The Cer stack was then pseudocolored to light blue for better visibility and was color merged with isolated GFP and tdT stacks to obtain the final triple color images.

Cells were manually tracked in FIJI by determining the x,y coordinates of the centers of nuclei. Tracking did not include the z dimension since cells rarely moved between z-sections during imaging sessions. The strong brightness of the H2BCer fluorescence enabled tracking of nuclei of differentiated hair shaft cells which were identified by anatomical location and extreme ovoid nuclear shape. Movement of DPs were measured by determining the boundaries of round DP clusters made by the surrounding epithelial or DS cells and weak H2BGFP fluorescence. Movements of cells and structures were standardized to the relative movement compared to the average movement of tracked ORS cells of each respective follicle. Any cells that underwent apoptosis during imaging were not included in movement quantifications.

For in vivo contraction inhibition during intravital 2-photon imaging, 10 μl DMSO was applied to imaging region and then imaging was acquired for 2 hours. Then with the imaging apparatus lifted off the skin, 10 μl of 1 mM ML7 HCL (Tocris) in DMSO was applied to the same region and let absorb for 5 minutes. 10 minutes were then allotted to reset the imaging

apparatus, locate the same imaging field and readjust for slight changes in z planes, and then resumed imaging for an additional 2 hours.

In vitro intracellular Ca^{2+} and contraction assays

Acan^{tdT} mice were injected with tamoxifen (0.15 g/kg i.p.) at P6 and P7 to fluorescently label DS. Single cell suspensions were obtained from P8 back skins using a dispase/collagenase digestion procedure as described for flow isolations and plated to 24-well plates. For contraction assays, cells were plated to pre-coated Matrigel (Corning 1:50) plates. Cells were grown in DMEM (Gibco) containing 10% bovine calf serum (HyClone) and were incubated at 37°C with 5 % CO_2 for 24-48 hours to allow for attachment. Cells were then incubated in Krebs buffer + glucose for 1 hour prior to assays. Both assays were conducted on an inverted DM6000 microscope with a live cell chamber set to 37° C with 5 % CO_2. DS cells were identified and selected by tdT fluorescence. Ca^{2+} assays were performed using the Fluo-8 No wash Calcium Assay Kit (AAT Bioquest). Fluorescence was quantified in FIJI by averaging the signal of three 25 x 25 μm areas per cell in the cell periphery. Cell surface areas during contraction assays were measured in FIJI by quantifying areas of thresholded fluorescence signal exclusive of cell-occupied areas.

Ex vivo hair follicle contraction assay

Hair follicles were microdissected from P8 back skin under a Leica S6E stereomicroscope in PBS and collected in 24-well plates. Media was then changed to Krebs buffer + glucose with or without 200 μM ML7 HCl (Tocris) and incubated for 1 hour at 37° C. Single follicles were then transferred to a 6 cm petri dishes immersed in Krebs buffer + glucose and immobilized by embedding the hair shaft tips in a 5 x 5 mm piece of parafilm. Follicles were then imaged under brightfield illumination on a Leica inverted DM6000 microscope in an enclosed live cell chamber at 37° C with 5 % CO_2. Images were taken with a 10X air lens with time intervals of 10 seconds. During imaging, media was exchanged for Krebs buffer + glucose with KCl supplanting NaCl and follicles were refocused when necessary, which took a duration of no more than 10 seconds. Measurements of follicle width at each time point were made in FIJI at three separate locations of the follicle isthmus located above the bulb and averaging. Presented data points and statistics were performed on the means of biological replicates each consisting of technical triplicates of width measurements.

In vivo contraction inhibition

Patches of lateral back skin measuring 1 x 1 cm of P13 mice were clipped and then shaved with a razor blade until no external hair shafts within patches remained. Vehicle-only control DMSO or ML7 HCl (Tocris) dissolved in an equal volume of DMSO (1 mM in 20 μl) was pipetted onto hairless patches and locally rubbed into the skin using a glass rod until visibly dry. Topical applications were performed twice daily from P13 to P19, once in the morning and once in the evening separated by 12 hours. Pieces of back skins including treated areas were then harvested at P20 for downstream analysis.

Statistics and reproducibility

Data are represented as percentages, whisker plots, bar plots, or line plots with error bars or boundaries as mean ± s. d. Two-tailed, unpaired Student's t-test was used to analyze data sets with two groups. ANOVA with Benjamini-Hochberg correction for multiple hypothesis testing

was performed to generate DEGs from RNA sequencing. Generation of data plots and statistical analyses were performed using Microsoft Excel, MATLAB (MathWorks), or Origin 2019 (OriginLab). No statistical method was used to predetermine sample sizes. *P*-values < 0.05 were designated as significant and symbolized in figure plots as $*P < 0.05$, $**P < 0.01$, $***P < 0.001$, $****P < 0.0001$ with precise values supplied in figure legends.

Figures, Tables, and Movie Captions

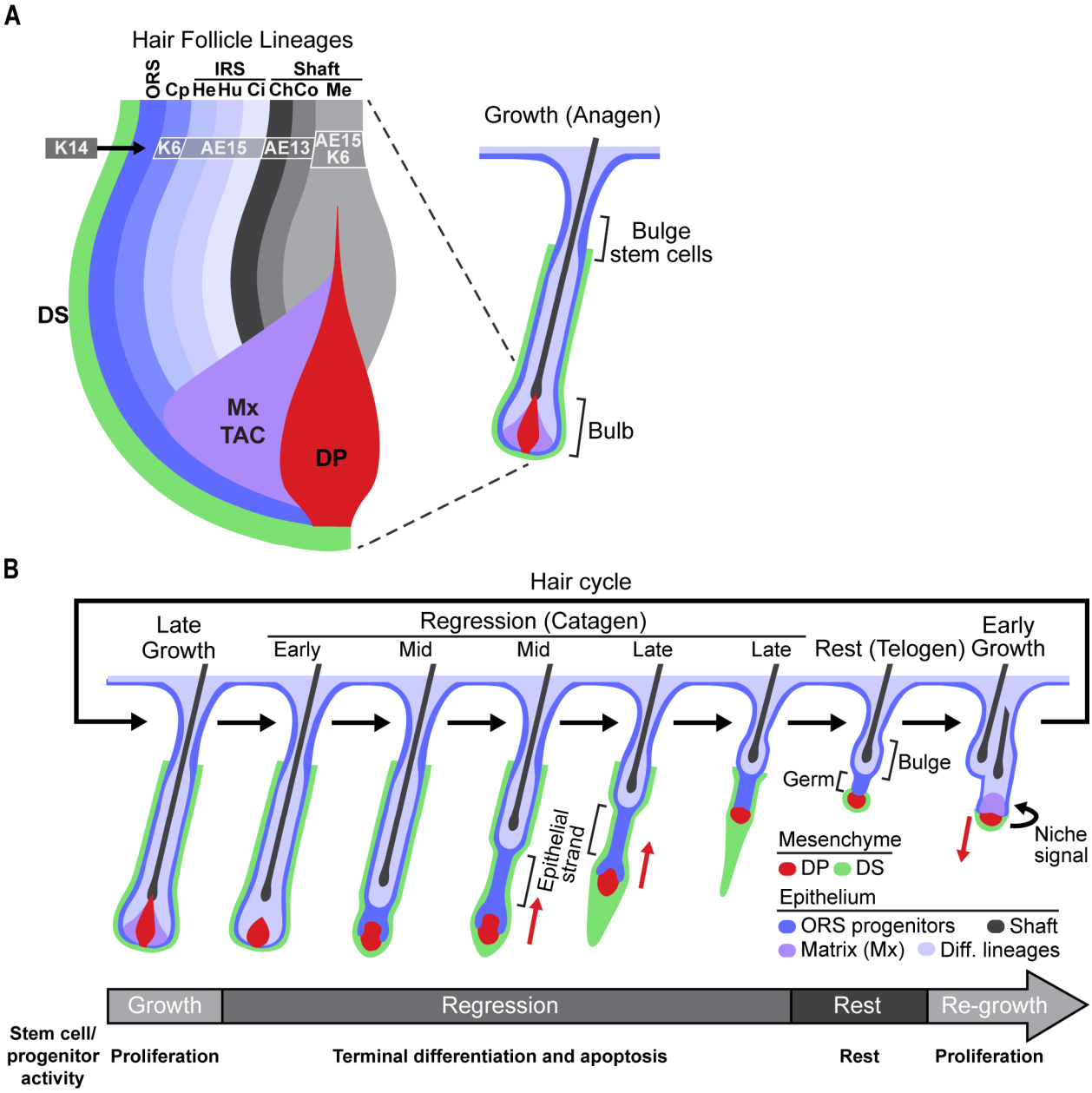

Fig. S1. The hair follicle cycle of dynamic stem cell niche reorganization. (**A**) Schematic of the hair follicle bulb and its epithelial and mesenchymal lineages during anagen growth. In the mesenchymal compartment, the dermal sheath (DS) forms the outermost casing of the follicle and the central dermal papilla (DP) at the base is engulfed by epithelial matrix (Mx) progenitors. The outer root sheath (ORS), the outermost layer of epithelium contains slow cycling multipotent progenitors. Mx progenitors abutting the DP consist of rapidly dividing transit amplifying cells (TAC) that produce progeny that differentiate into cells of the outgoing shaft and its channel. Distinct markers highlight epithelial lineages: K14 for ORS; K6 for companion layer (Cp) and shaft medulla (Me); AE15 for Henle's layer (He), Huxley's layer (Hu), and cuticle (Ci) of the

inner root sheath (IRS) and shaft medulla (Me); AE13 for shaft cuticle (Ch) and cortex (Co). (**B**) Schematic of the hair cycle with focus on catagen regression. During catagen onset, matrix progenitors cease proliferation and deplete through terminal differentiation. Throughout mid- and late-catagen, ORS progenitors undergo large-scale pruning by apoptosis. During regression, the shaft and DP niche are translocated upward through an unknown mechanism. Throughout the entirety of catagen, the DS encapsulates the follicle. In late catagen, the DS extends below the DP forming an empty sleeve. At the conclusion of catagen, the DP niche resides adjacent to the stem cell reservoir, an essential position vital for the relay of short-range activating niche signals to the stem cells for induction of hair regeneration and the start of a new cycle.

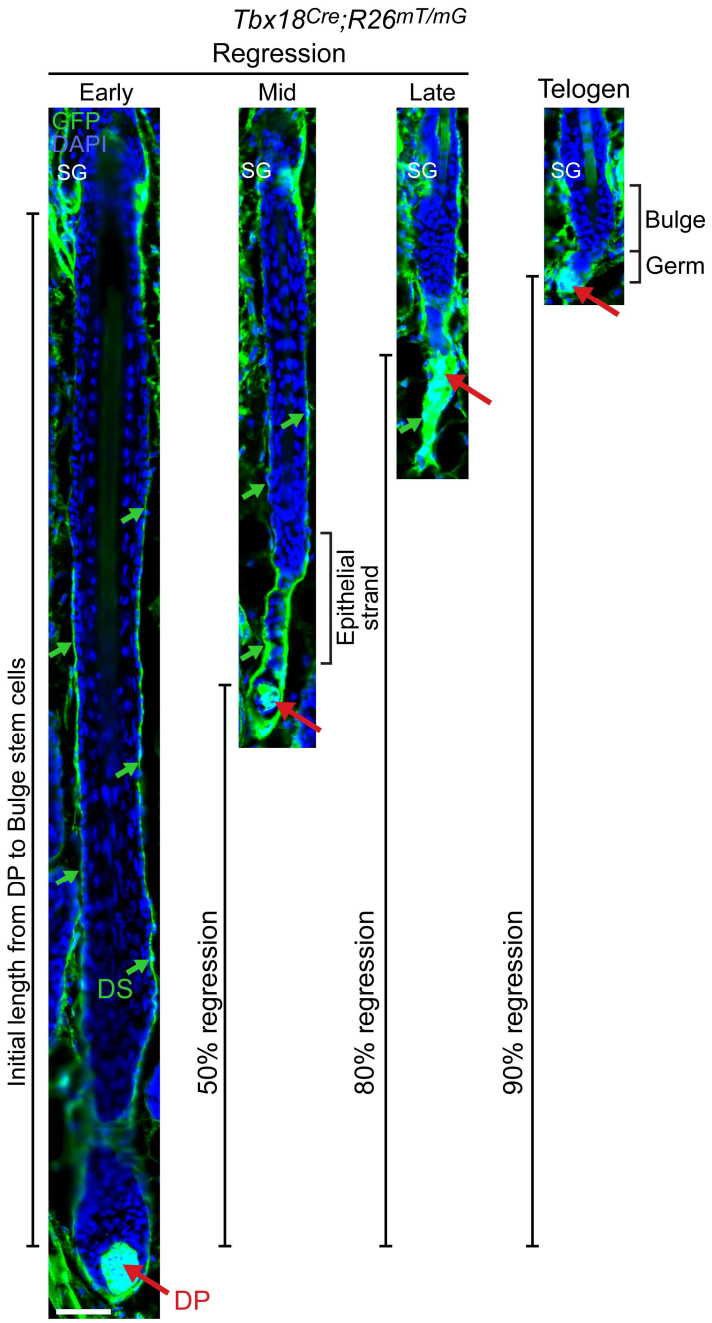

Fig. S2. Drastic homeostatic follicle remodeling and niche relocation to the stem cell reservoir during catagen regression. Histological section of *Tbx18*^{Cre};*R26*$^{mT/mG}$ back skin follicles. Mesenchymal populations including DP (red arrows) and DS (green arrows) are marked by membrane GFP. During catagen regression, the DP niche relocates a distance of ~90% of the follicle length (between DP and sebaceous gland, SG). At the beginning of regression, matrix progenitors degenerate, and the DP niche (now rounded appearance) is only partially engulfed. During mid-regression, the DP is connected to the upper follicle via the regressing epithelial strand. The thin DS layer becomes notably thicker around the epithelial strand and DP. During final regression, the hair shaft reaches its final position and the DP is separated from the stem cell reservoir only by the epithelial strand. The DS forms a dense

trailing empty sleeve below the DP. After the conclusion of regression (telogen = rest), the DP niche resides adjacent to the stem cell reservoir. Cell nuclei are highlighted by DAPI. Scale bar, 50 μm.

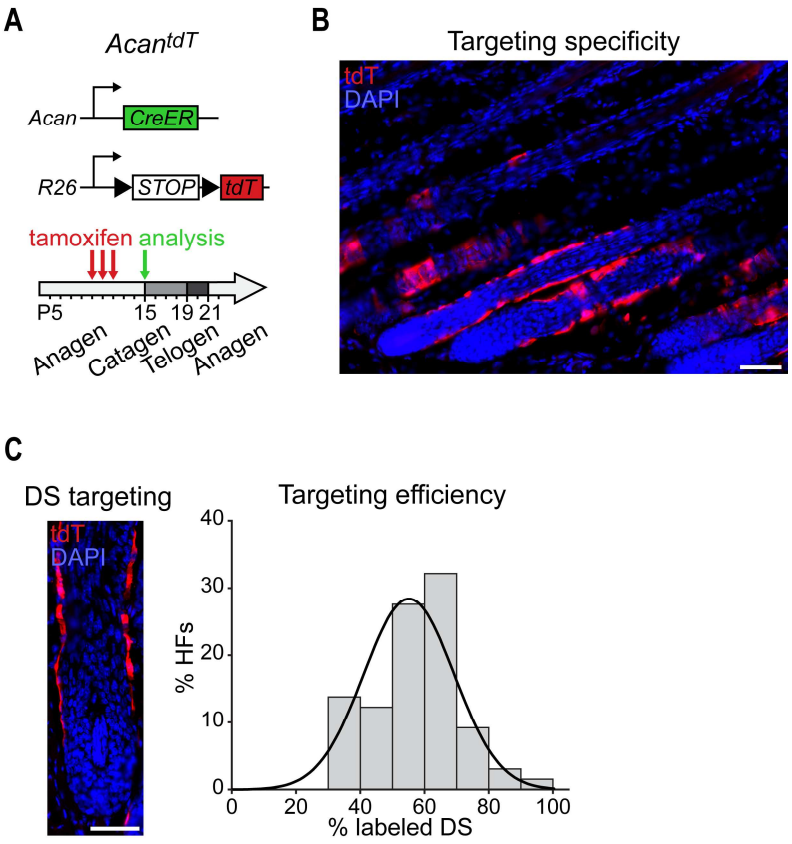

Fig. S3. Highly selective and inducible DS targeting with *Acan*^{CreER}. (**A**) Schematic of fluorescence reporter of dermal sheath genetic targeting with *Acan*^{CreER};*R26*$^{LSL\text{-}tdTomato}$ (*Acan*^{tdT}). (**B**) Fluorescence microscopy for tdT expression in back skin after induction with tamoxifen from P10-12 and analysis at P15. (**C**) Quantification of follicles with DS labelling. Data bars are means of each bin; n = 65 follicles from 3 mice. Line is normal distribution fit of data. Scale bars, 50 μm.

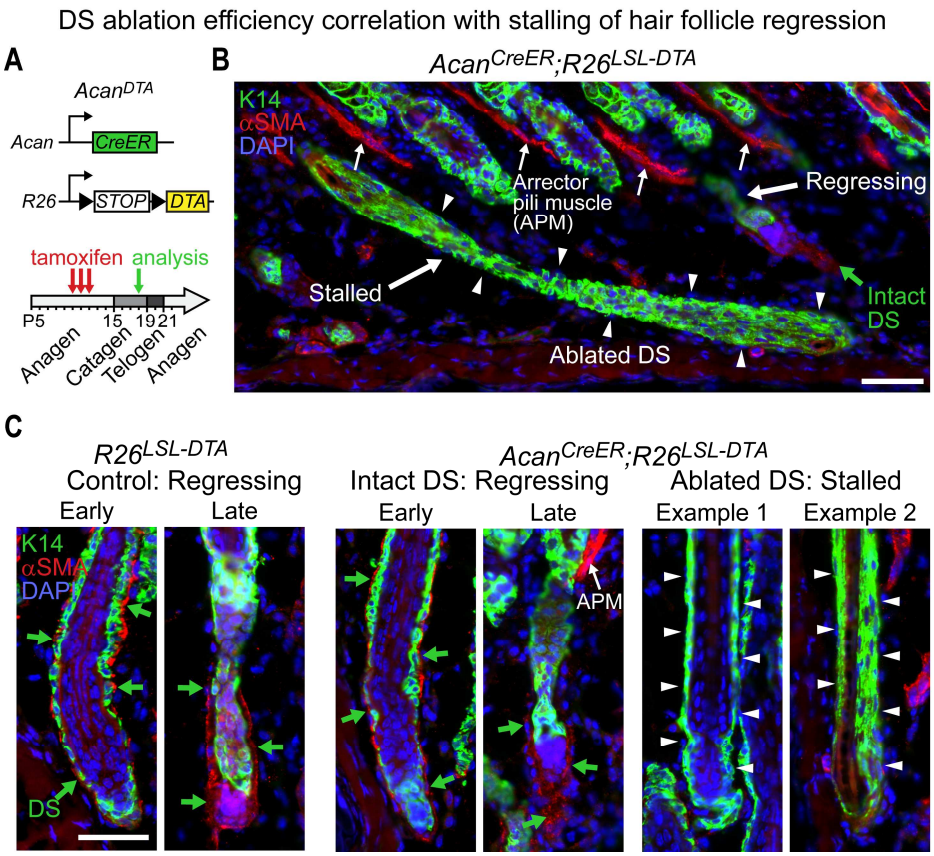

Fig. S4. Complete DS ablation in stalled and incomplete ablation in regressing follicles. (**A**) Schematic of cytotoxic ablation of DS during catagen with analysis at late catagen (P18). (**B**, **C**) Immunofluorescence for K14 identifies stalled versus regressing follicles in same section and αSMA shows presence of intact DS (green arrows) in all control (*R26*$^{LSL\text{-}DTA}$) and regressing follicles of *Acan*^{CreER};*R26*$^{LSL\text{-}DTA}$. Stalled follicles notably have complete DS ablation (arrowheads). Scale bars, 50 μm.

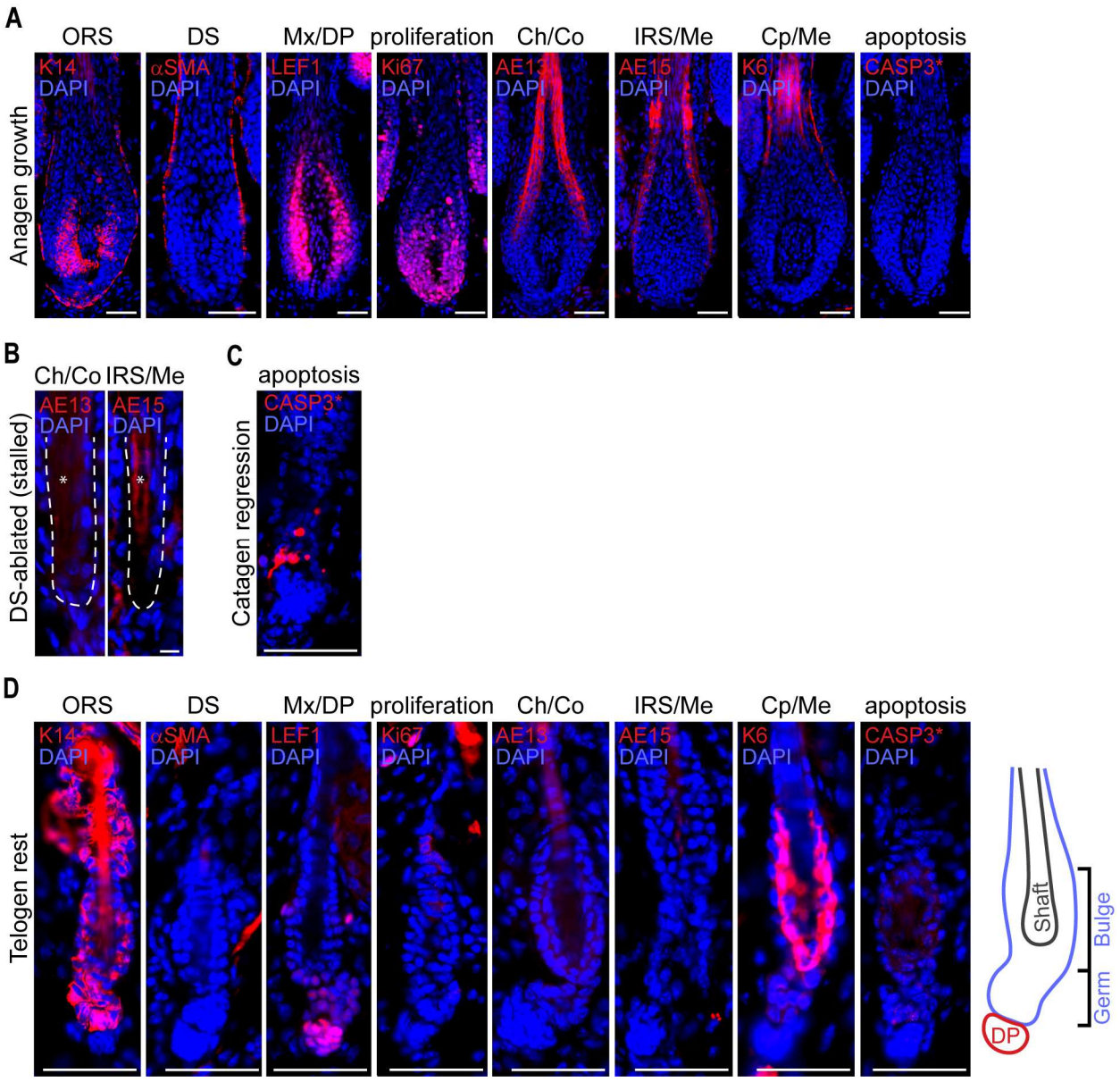

Fig. S5. Immunofluorescence of lineage, proliferation, and apoptosis markers. Control immunofluorescence of wild-type anagen (P8), catagen (P18), and telogen (P20) hair follicles. (**A**) Outer root sheath progenitors during anagen are $K14^{+}$. The DS is marked by αSMA. Matrix progenitors express LEF1 and are $Ki67^{+}$ indicative of proliferative status. LEF1 is also moderately expressed in DP. Differentiated epithelial lineage markers are detectable in inner root sheath (IRS), AE15; shaft cortex (Co) and cuticle (Ch), AE13; shaft medulla (Me), AE15 and K6; and companion layer (Cp), K6. Cell death by apoptosis is undetectable (active caspase 3, CASP3*). (**B**) Stalled follicles lack differentiating cuticle (Ch), cortex (Co), medulla (Me) of hair shaft, and inner root sheath (IRS) indicating that differentiation has finished during the early steps of catagen. (**C**) Progenitor pruning by apoptosis is detectable by activated CASP3*. (**D**) Proliferation, differentiation, and apoptosis markers are absent in telogen follicles. Only K6 marks the inner bulge cells of telogen follicles. $αSMA^{+}$ DS is absent during telogen. K14 is retained in bulge and germ stem cells. Scale bars, 50 μm (**A**, **C**, **D**) and 10 μm (**I**).

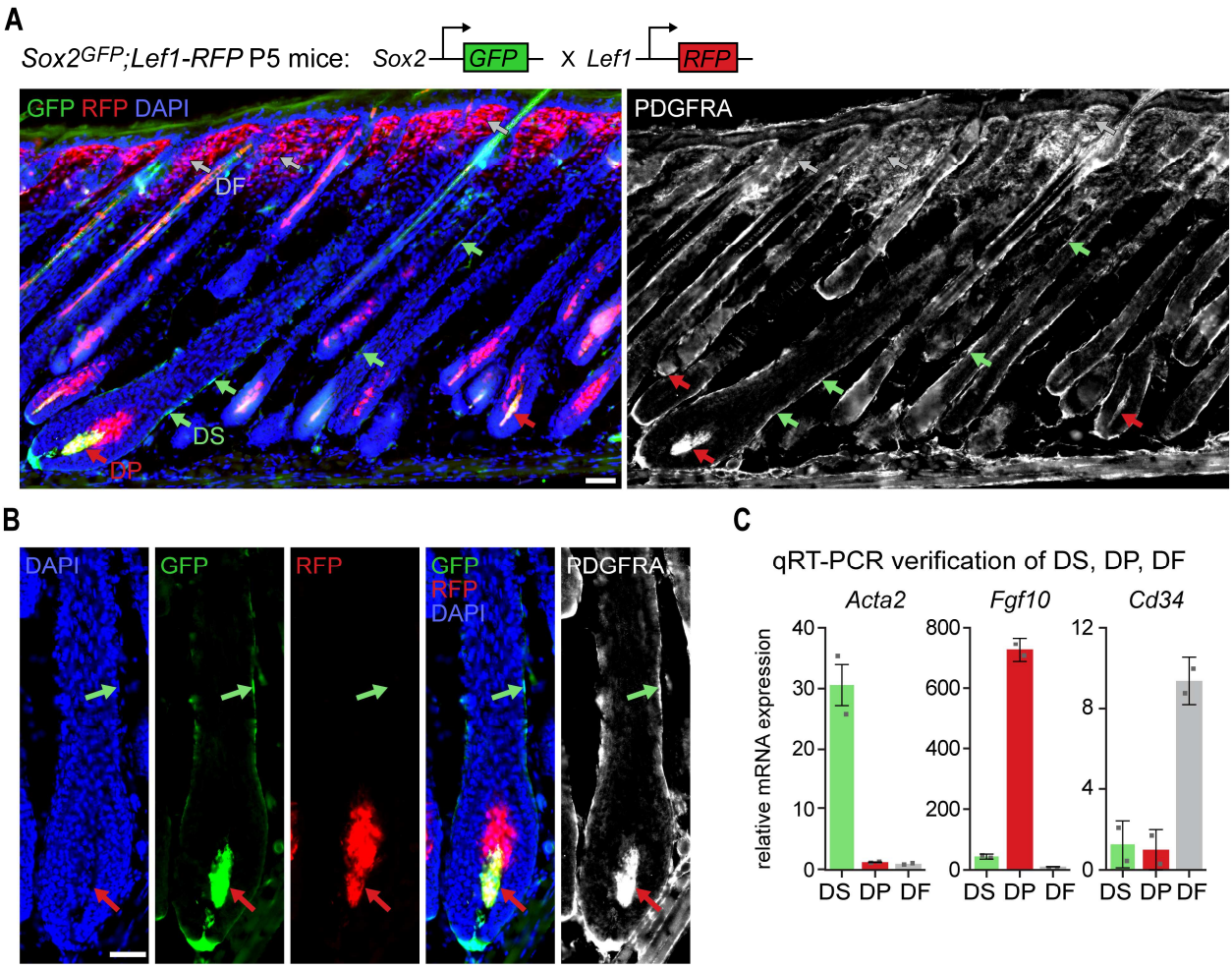

Fig. S6. DP, DS, and dermal fibroblast (DF) labeling for cell isolation. (**A**) *Sox2*^{GFP}*;Lef1*^{RFP} mice and PDGFRA immunofluorescence for cell isolations. GFP marks DP (red arrows) and DS (green arrows). DF (grey arrows) and DP have robust RFP fluorescence, which is absent in DS cells. DP and DS can be further distinguished from other GFP^{+} skin populations by PDGFRA staining. (**B**) Individual fluorescence channels and merge. (**C**) qRT-PCR verification of sorted populations by known marker genes performed on biological duplicates. Scale bars, 50 μm.

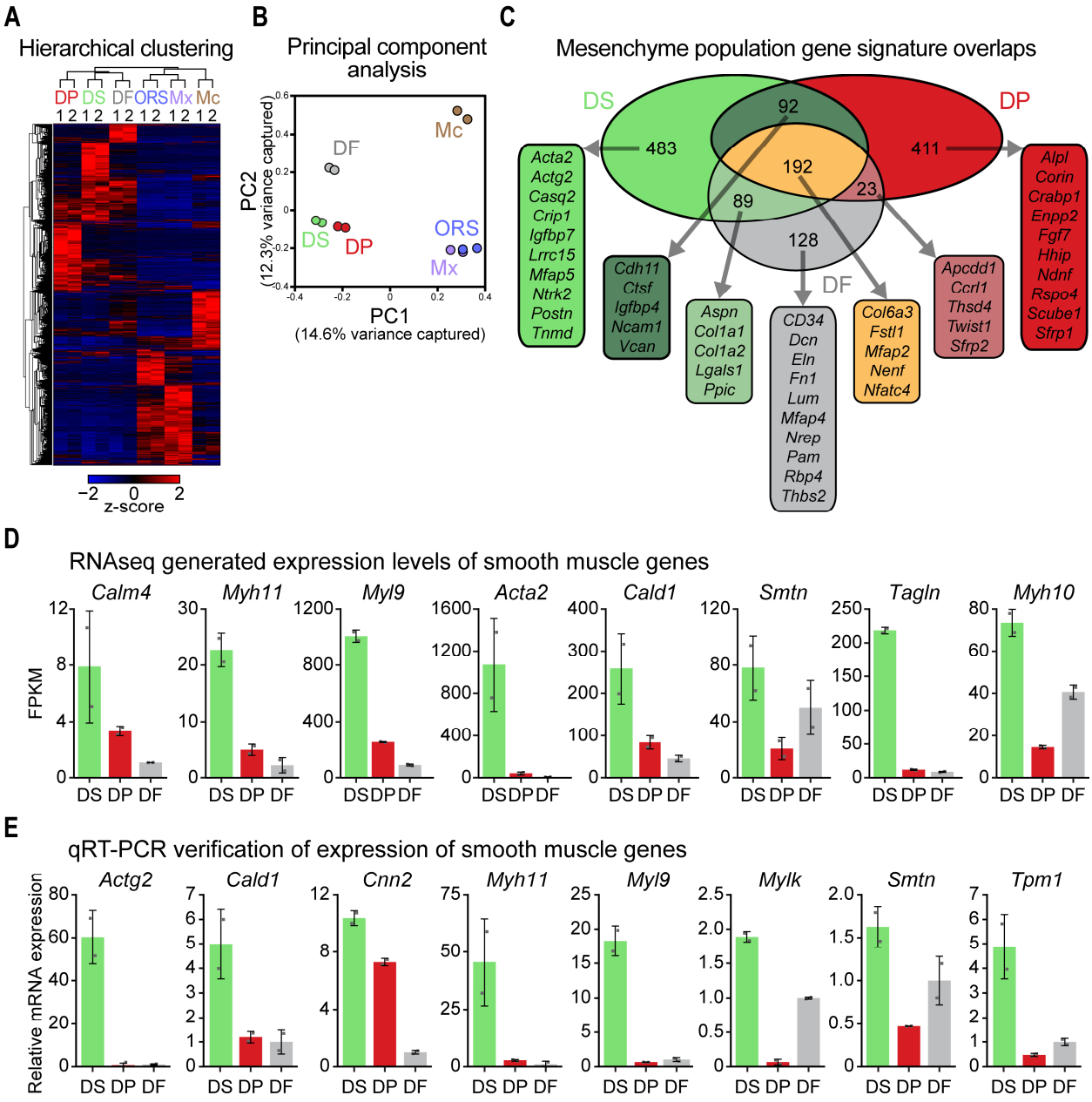

Fig. S7. RNA sequencing analysis and smooth muscle gene enrichment in DS. (**A**) Hierarchical clustering of DS, DP, DF, ORS, matrix (Mx), and melanocytes (Mc) using all differentially expressed genes identified by ANOVA (FDR < 0.05). Biological duplicates of sorted populations cluster together. DS, DP, and DF and ORS and Mx cluster together indicative of lineage relatedness. (**B**) Principal component analysis using all differentially expressed genes. DS, DP, and DF cluster together apart from ORS, Mx, and Mc, and DS and DP cluster closer than DF. Mc cluster separate from other populations. (**C**) Signature gene analysis reveals 483 DS signature genes. (**D**) Expression levels of smooth muscle genes from RNA sequencing represented as fragments per kilobase per million mapped reads (FPKM). (**E**) qRT-PCR verification of smooth muscle gene expression in DS. Data are mean ± s.d.

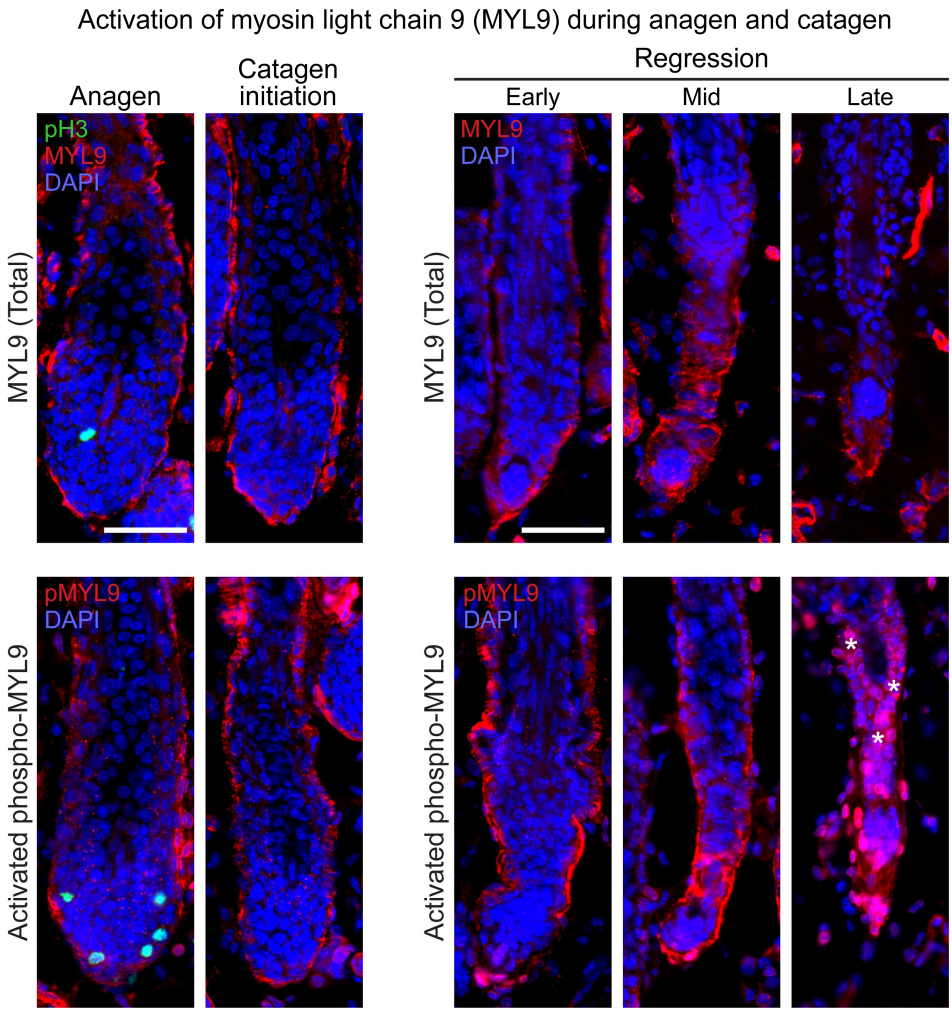

Fig. S8. Contraction is active throughout the entire DS from anagen through catagen. Immunofluorescence for the regulatory myosin light chain 9 (MYL9) and the activated phosphorylated form pMYL9 in anagen, catagen initiation, and early, mid, and late regression. Phospho-histone H3 staining for proliferating mitotic cells in matrix distinguished late anagen (labeled cells) and catagen initiation (no labeled cells). Early, mid, and late regression were determined by follicle morphology. Asterisks denote non-specific staining of phospho-MYL9 in the epithelium during late regression (regions without total MYL9). Scale bars, 50 μm.

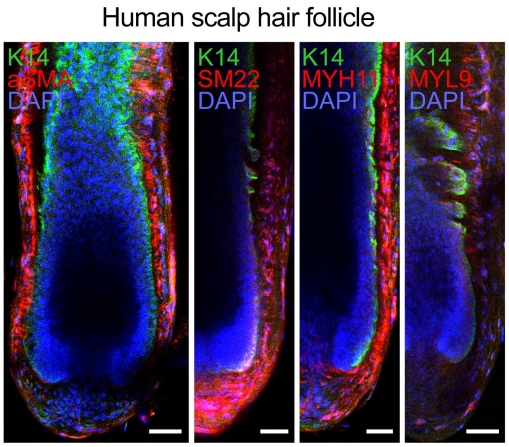

Fig. S9. Smooth muscle protein expression in the DS of human hair follicles.
Immunofluorescence of smooth muscle proteins in human scalp follicles. Scale bars, 50 μm.

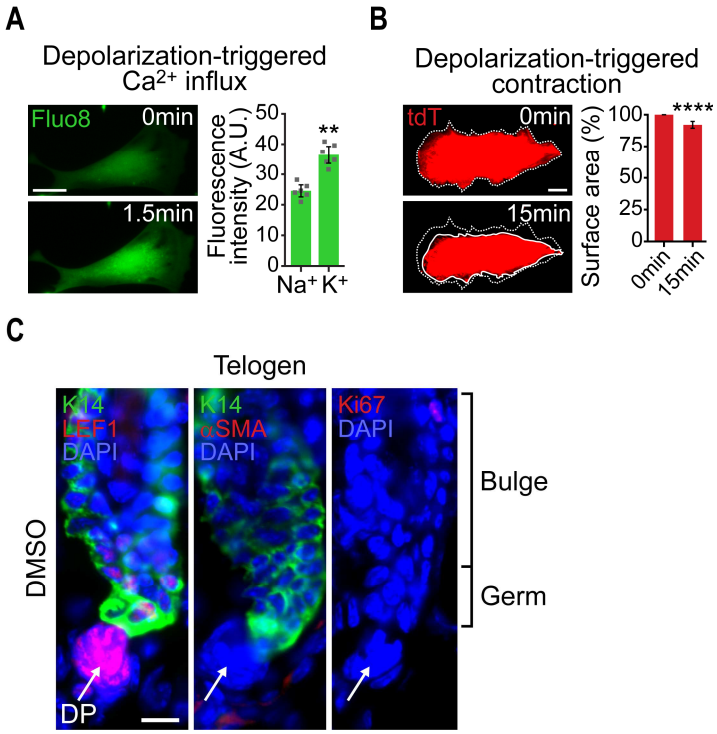

Fig. S10. DS cells can contract *in vitro* and DS-mediated hair follicle contraction is required for regression *in vivo*. (**A**) High K^+ membrane depolarization activates Ca^{2+} influx in isolated DS cells (Fluo8 indicator). $n = 6$. Data bars are mean ± 95% C.I. $^{**}P = 0.002$, paired two-tailed *t*-test. (**B**) High K^+ membrane depolarization triggers DS contraction and surface area reduction in cells grown on matrigel. n = 35. Data bar is mean ± 95% C.I. $^{****}P < 10^{-4}$, paired two-tailed *t*-test. (**C**) Immunofluorescence for LEF1, proliferation marker Ki67 and αSMA demonstrated full regression of follicles into telogen in DMSO treated control skin region. K14 marks bulge and germ stem cells, and LEF1 marks the relocated, adjacent DP. Absence of Ki67 in the stem cells confirms telogen quiescent state. $αSMA^+$ DS is absent in the telogen follicle. Scale bars, 10 μm (**A**, **B**) and 50 μm (**B**).

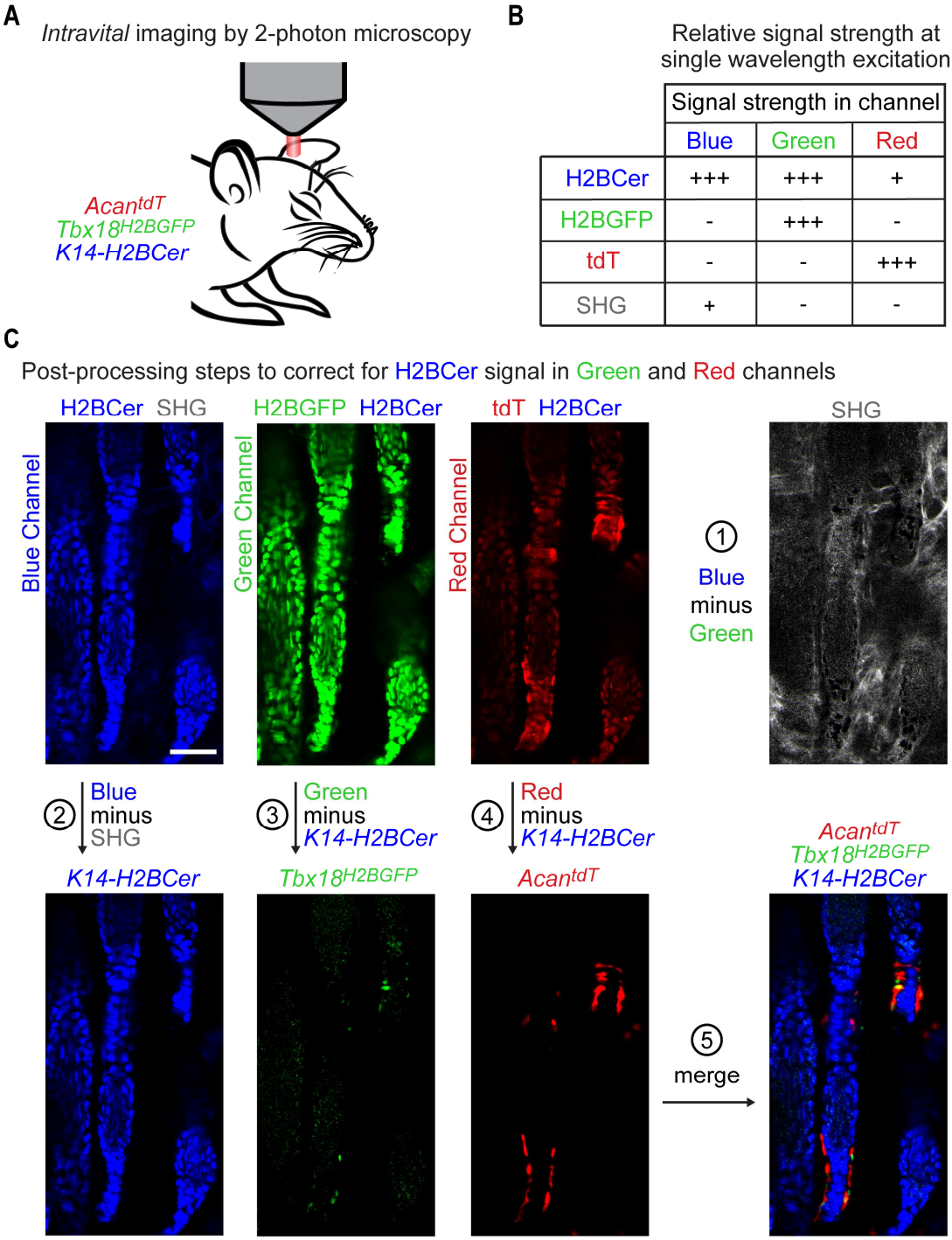

Fig. S11. Post-processing of triple-color 2-photon imaging. (**A**) *Intravital* imaging setup of live mice. (**B**) Table of fluorescence signal strength of fluorophores in each channel using a single 900 nm excitation wavelength. (**C**) Steps of fluorophore signal isolation. (1) Isolate second harmonic generation (SHG) signal in raw blue channel data by subtracting green channel from blue channel. (2) Isolate H2BCer-only signal by subtracting isolated SHG from raw blue channel. (3 and 4) Isolate H2BGFP and tdT signals by subtracting H2BCer-only signal from raw

green and red channels, respectively. (5) Merge isolated tdT, H2BGFP and H2BCer signals and pseudo-color H2BCer to light blue for visibility. Scale bar, 50 μm.

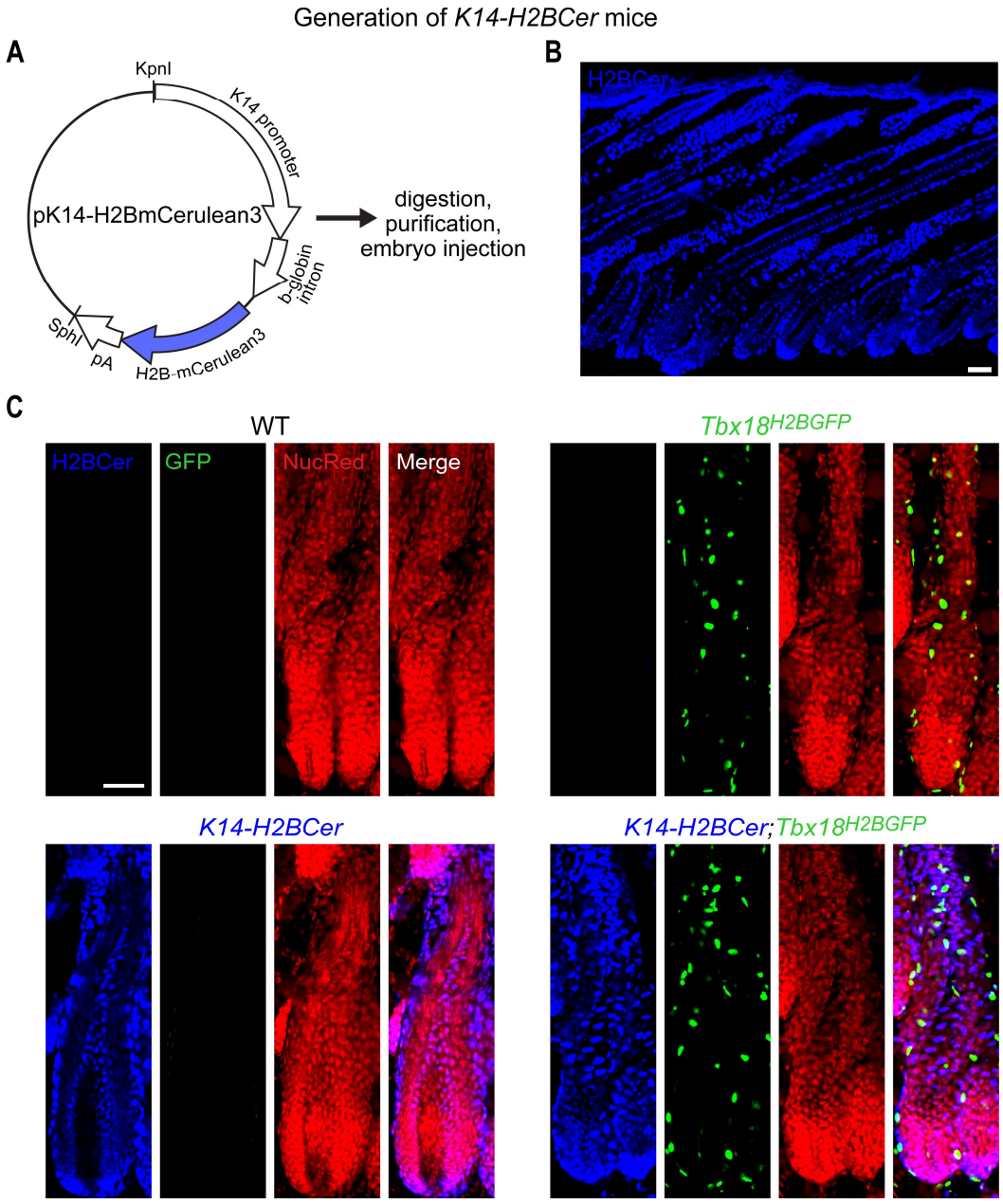

Fig. S12. Generation of *K14-H2BCer* fluorescence reporter mice. (**A**) Schematic of transgenesis strategy. The coding sequence for *H2B-mCerulean3* fusion protein was inserted into plasmid vector containing *K14* promoter, b-globin intron, and polyA (pA). (**B**) Cerulean fluorescence is restricted to epithelial cells in skin epidermis and hair follicles. (**C**) Distinct fluorescence of Cerulean (nuclei of epithelial cells) and GFP (nuclei of DS and other mesenchymal cells) in *Tbx18*^{H2BGFP};*K14-H2BCer* anagen back skin. Far-red NucRed 647 highlighted all nuclei. Scale bars, 50 μm.

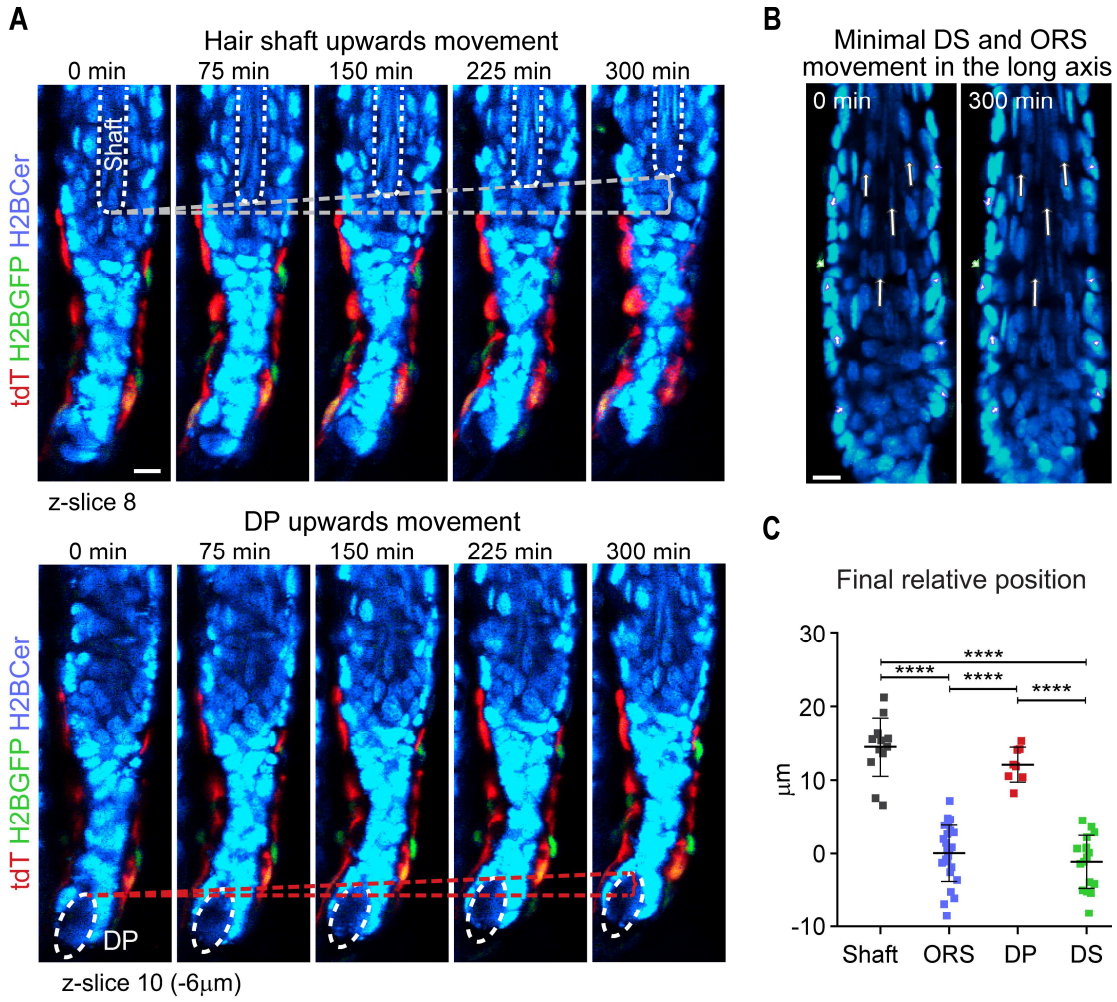

Fig. S13. Dynamic movements of hair follicle populations during regression. (**A**) *Intravital* 3D time-lapse imaging of catagen regression in live mice. Triple-fluorescent *Acan*^{tdT}*;Tbx18*^{H2BGFP}*;K14-H2BCer* reporter follicles were live-imaged for 5 hours. Time courses of two optical slices capturing shaft (z-slice 8) and DP (z-slice 10) movements (slices are separated by 6 μm). Steady upward movements of shaft and DP are outlined by sloped grey and red dashed lines, respectively. (**B**) Cell tracking for quantifying cell movements during regression. DS and ORS show minimal movement in the long axis. Bases of arrows are at starting position and tips of arrows are at ending position of 5-hour cell tracking. (**C**) (**F**) Final relative cell movement. ****$P < 10^{-8}$, unpaired two-tailed *t*-test. Arrows are starting and ending positions of 5-hour tracking. Scale bars, 10 μm.

Gene	Forward Primer	Reverse Primer
Acta2	CCCTCCAGAACGCAAGTACTC	GCGCTGATCCACAAAACGTTC
Fgf10	ATTTCCCCCTGTATGCATCCTAAC	TTCCCACGGAGGCAGAACTC
Dpp4	GCATGAATTGCAAACGTGGCAG	TGGATACTGCTGCACATGGTGA
Actg2	TCCTTCATTGGCATGGAGTCAG	TGCCTCATCATACTCTGGCTTG
Cald1	GACTCCGCCGAAAATGAGACA	GTTCCCCATCCCCTTCTATTTTG
Cnn1	CCACCCGCACAACTACTACAACTC	AATGGGGCAGGGGTCAGG
Myh11	CGCTCGGGACTCAGACTTCAA	CTGTGGCACCCATTCATGTAACTTC
Myl9	ATGGGCGACCGATTCACG	TCGTCACGGGGAGGGTAGAG
Mylk	GAAAAGCCCCATGTGAAACCTTAT	TTGCCGTCTTCGTCGTAGTCTATC
Smtn	GCCGCAGCTCCTGGATAC	CAGGCGGTGTGAGCAGAGTG
Tpm1	ATCGGGTGCGGATTGGTG	GCTCGCCCCACTGAGTC

Table S3. qRT-PCR primer sequences. List of primer sequences used for qRT-PCR.

Movie S1. *Ex vivo* hair follicle contraction. Time-lapse recording of follicle width constriction induced by high K^+ spike. Note significant reduction in width above the bulb after three minutes of high K^+ (arrows). Also see Figs. 3D, F.

Movie S2. *Ex vivo* hair follicle contraction blocked by ML7. Time-lapse recording of follicle during high K^+ spike in the presence of MLCK inhibitor, ML7. ML7 preincubation blocked contraction with no discernible reduction in follicle width. Also see Figs. 3E, F.

Movie S3. Dynamic cell movements of hair follicle populations during regression captured by *intravital* imaging. Time-lapse recording of hair follicle regression visualized by tdT, H2BGFP and H2BCer in *Acan*^{tdT}*;Tbx18*^{H2BGFP}*;K14-H2BCer* reporter mice. The 5-hour live imaging captures shaft (grey) and DP (red) upward movements concurrent with DS centripetal constriction movement at the club-epithelial strand bottleneck (green arrows).

Additional Table S1 (separate file). Gene list of DS, DP, DF signatures and overlaps. Gene identities from Venn diagram in Fig. 2D.

Additional Table S2 (separate file). Gene list of "Regulation and Process of Smooth Muscle Contraction" category. List of gene set of smooth muscle contraction and regulation components used in Gene Set Enrichment Analysis in Fig. 2F.

Methods References

35. P. Ellis *et al.*, SOX2, a persistent marker for multipotential neural stem cells derived from embryonic stem cells, the embryo or the adult. *Dev. Neurosci.* **26**, 148–65 (2004).

36. M. D. Muzumdar, B. Tasic, K. Miyamichi, L. Li, L. Luo, A global double-fluorescent Cre reporter mouse. *Genesis*. **45**, 593–605 (2007).

37. S. P. Henry *et al.*, Generation of aggrecan-CreERT2 knockin mice for inducible Cre activity in adult cartilage. *Genesis*. **47**, 805–14 (2009).

38. L. Madisen *et al.*, A robust and high-throughput Cre reporting and characterization system for the whole mouse brain. *Nat. Neurosci.* **13**, 133–40 (2010).

39. D. Voehringer, H.-E. Liang, R. M. Locksley, Homeostasis and effector function of lymphopenia-induced "memory-like" T cells in constitutively T cell-depleted mice. *J. Immunol.* **180**, 4742–53 (2008).

40. L. Li, D. D. Ginty, The structure and organization of lanceolate mechanosensory complexes at mouse hair follicles. *Elife*. **3**, e01901 (2014).

41. C. Trapnell, L. Pachter, S. L. Salzberg, TopHat: discovering splice junctions with RNA-Seq. *Bioinformatics*. **25**, 1105–11 (2009).

42. B. Langmead, S. L. Salzberg, Fast gapped-read alignment with Bowtie 2. *Nat. Methods*. **9**, 357–9 (2012).

43. C. Trapnell *et al.*, Transcript assembly and quantification by RNA-Seq reveals unannotated transcripts and isoform switching during cell differentiation. *Nat. Biotechnol.* **28**, 511–5 (2010).

44. C. M. Pineda *et al.*, Intravital imaging of hair follicle regeneration in the mouse. *Nat. Protoc.* **10**, 1116–30 (2015).